J. Plasma Phys. (2026), *vol*. 92, E88 © The Author(s), 2026. Published by Cambridge University Press.
This is an Open Access article, distributed under the terms of the Creative Commons Attribution licence (https://creativecommons.org/licenses/by/4.0/), which permits unrestricted re-use, distribution and reproduction, provided the original article is properly cited. doi:10.1017/S0022377826101342

Relativistically strong electromagnetic waves in magnetised plasmas

Maxim Lyutikov[1]

[1]Department of Physics and Astronomy, Purdue University, 525 Northwestern Avenue, West Lafayette, IN 47907-2036, USA

Corresponding author: Maxim Lyutikov, lyutikov@purdue.edu

(Received 24 September 2025 UTC; revision received 9 December 2025 UTC; accepted 23 January 2026 UTC)

Using a two-fluid approach, we consider the properties of relativistically nonlinear (arbitrary a_0), circularly polarised electromagnetic waves propagating along a magnetic field in electron–ion and pair plasmas. Dispersion relations depend on how wave intensity scales with frequency, e.g. $a_0(\omega)$. For superluminal branches, the nonlinear effects reduce the cutoff frequency, while the general form of the dispersion relations $\omega(k)$ remains similar to the linear case. For subluminal waves, whistlers and Alfvén, a new effect appears: dispersion curves effectively terminate at finite ω^*-k^*, where the group velocity becomes zero. Qualitatively, subluminal modes with fluctuating electric field larger than the guide field, $E_w(\omega) \geqslant B_0$, cannot propagate. In extended systems, e.g. within magnetospheres of neutron stars, this leads to opening of the magnetosphere by a strong wave.

Key words: astrophysical plasmas, plasma nonlinear phenomena

1. Introduction

The dynamics of nonlinear waves in plasmas is a classical problem in plasma physics (Akhiezer & Polovin 1956; Clemmow 1974; Akhiezer *et al*. 1975). Recently it became important for astrophysical fast radio bursts (FRBs) (Lorimer *et al*. 2007; Cordes & Chatterjee 2019; Petroff, Hessels & Lorimer 2022). Such FRBs are millisecond-long bursts of radio emission coming from approximately halfway across the Universe. At the peak the (isotropic-equivalent) luminosity (in radio) exceeds billions of solar luminosity (in optical) (Petroff *et al*. 2022).

An important astrophysical hint comes from the observations of correlated radio and X-ray bursts from ultra-magnetised neutron stars (Bochenek *et al*. 2020; CHIME/FRB Collaboration *et al*. 2020). This established the FRB–magnetar connection. If the emission originates in the magnetospheres, the laser nonlinearity parameter in these settings can be as high as a staggering

$$a_0 = \frac{eE_w}{m_e c\omega} \sim 10^9, \tag{1.1}$$

where E_w is the electric field in the wave and ω is the wave frequency. Parameter regime $a_0 \geqslant 1$ defines relativistic nonlinearity of the wave.

In addition, the wave–plasma interaction may occur in the highly magnetised environment, in the regime when the guiding magnetic field strongly affects particle dynamics and laser–plasma interaction. Guide fields can be as strong as, or even exceed, the quantum magnetic field. In addition, plasma parameters are changing as the electromagnetic (EM) pulse propagates away from a neutron star (see e.g. Luan & Goldreich 2014; Lyubarsky 2014; Lyutikov, Burzawa & Popov 2016; Beloborodov 2021; Lyutikov 2021; Golbraikh & Lyubarsky 2023).

Astrophysical challenges of super-strong waves in plasmas connect to modern laser experiments. The interaction of intense laser beams with plasma is critical for the success of high-energy-density experiments, inertial confinement fusion and, eventually, inertial fusion energy. High-intensity colliding laser pulses also can lead to a new type of laboratory experiments by creating abundant electron–positron pair plasmas (Marklund & Shukla 2006; Bell & Kirk 2008; Ridgers *et al*. 2012; Zhang *et al*. 2020). This process, first discussed more than a decade ago, is becoming a reality.

In addition, for a pair plasma there are a number of principal differences between astrophysical and laboratory set-ups. (i) There are subluminal branches in astrophysical highly magnetised plasmas; waves are relativistically nonlinear. Modern lasers can in principle achieve $a_0 \geqslant 1$, but usually only in a very limited region of space (extended wave trains typically have $a_0 \leqslant 0$). (ii) Almost universally, in laboratory experiments waves are shone onto a plasma from outside, while in astrophysical settings nonlinear waves can be generated by particles already inside the plasma. These correspond to two different set-ups: boundary condition problem for waves falling from outside, and eigenmode problem for waves inside the plasma.

Finally, there are a number of limitations to numerical particle-in-cell (PIC) approaches. High-intensity EM waves with $a_0 \gg 1$ falling onto a pair plasma accelerate it ponderomotively to relativistic energies, and experiences modulational instability that leads to reflection (Lyutikov & Gurarie 2025; Tangtartharakul, Arefiev & Lyutikov 2025, these works exploring unmagnetised plasmas). Finally, setting up a subluminal wave already inside a plasma is highly non-trivial in PIC simulations, as all the codes (to the best of our knowledge) ignore the initial current created by the initial particle velocities (initial velocity is not used for current computation until the first update is done). This is especially problematic for subluminal waves, where $\nabla \times B \sim (4\pi/c)\, j$. An additional numerical complication of setting nonlinear waves inside a plasma involves the fact that velocity (current), magnetic field and electric field are all evaluated at different times. To set a correct self-consistent nonlinear wave inside a plasma then would involve subtle half-step corrections. These arguments demonstrate the usefulness of a purely theoretical approach.

In this paper, we address the basic properties of plasma in this new regime: dispersion relations of relativistically nonlinear waves. We consider a particular case of circularly polarised (CP), fully nonlinear EM waves propagating along a magnetic field. This regime allows, within the two-fluid approximation, a fully nonlinear treatment.

We employ a two-fluid (cold and collisionless) approach. An important advantage of the two-fluid treatment over the magnetohydrodynamics approach (e.g. Heyvaerts, Lehner & Mottez 2012) is that the current is calculated self-consistently from the dynamic equations for each species.

https://doi.org/10.1017/S0022377826101342 Published online by Cambridge University Press

2. Two-fluid model for relativistically nonlinear CP waves

The governing equations within the two-fluid model for relativistically nonlinear CP waves are exceptionally simple. They include just Maxwell's equations and transverse force balance:

$$\begin{aligned} \nabla \times \boldsymbol{B} &= 4\pi \boldsymbol{J} + \partial_t \boldsymbol{E}, \\ \boldsymbol{J} &= e(\boldsymbol{v}_p - \boldsymbol{v}_e)n, \\ d_t \boldsymbol{p}_{e,p} &= \mp \left(\boldsymbol{E} + \frac{\boldsymbol{p}_{e,p}}{\sqrt{1+p_{e,p}^2}} \times \boldsymbol{B} \right), \end{aligned} \tag{2.1}$$

where $\boldsymbol{p}_{e,p}$ are particle momenta; upper signs are for electrons. Equations are written in the common gyration frame (no axial motion).

This major simplification comes from the fact that for a fully relativistically nonlinear CP EM wave propagating along a magnetic field (in the z direction), the oscillations are harmonic (this is not true for linearly polarised waves), while density remains constant. This is a major observation underlying the present work.

Let us introduce a unit vector corresponding to the wave vector potential:

$$\boldsymbol{e}_w = \{\cos(\omega t - kz), -\sin(\omega t - kz), 0\}. \tag{2.2}$$

The motion of particles in the EM field (guide plus waves) consists of forced motion by the wave and free oscillations. Importantly, we are interested in forced oscillations due to the influence of the wave on particle motion. (Though this statement seems obvious, it is an important point in selecting the correct dispersion branches; see § 5.3.) In this case, for CP waves, the momentum of the particles is parallel to the wave magnetic field (aligned or counter-aligned). Thus we can write

$$\boldsymbol{p}_{e,p} = a_{e,p}\boldsymbol{e}_w. \tag{2.3}$$

The relations (2.1) then give

$$n^2 - 1 = \left(\frac{a_p}{\sqrt{1+a_p^2}} - \frac{a_e}{\sqrt{1+a_e^2}} \right) \frac{\omega_p^2}{a_0\omega^2} = (\tanh\chi_p - \tanh\chi_e)\frac{\omega_p^2}{a_0\omega^2}, \tag{2.4}$$

$$a_0 = \left(\frac{f_B}{\sqrt{1+a_p^2}} - 1 \right) a_p = \tanh\chi_p(f_B - \cosh\chi_p), \tag{2.5}$$

$$a_0 = \left(\frac{f_B}{\sqrt{1+a_e^2}} + 1 \right) a_e = \tanh\chi_e(f_B + \cosh\chi_e), \tag{2.6}$$

$$a_{p,e} \equiv \sinh(\chi_{e,p}), \tag{2.7}$$

where $n = k/\omega$, frequency parameter $f_B = \omega_B/\omega$ and we introduced rapidity $\chi_{e,p}$ (so that $v_{e,p} = \tanh(\chi_{e,p})$).

In (2.7) the plasma frequency

$$\omega_p^2 = \frac{4\pi e^2 n}{m_e} \tag{2.8}$$

https://doi.org/10.1017/S0022377826101342 Published online by Cambridge University Press

is defined with respect to the density of each component (e.g. in pair plasma the relevant terms in the dispersion relations are $\propto 2\omega_p^2$). The cyclotron frequency

$$\omega_B = \frac{eB}{m_e c} \tag{2.9}$$

is positively defined; the signs of charges are explicitly taken into account.

In what follows, whenever dimensionless momentum or energy appear, they should be understood in terms of $p/(m_e c)$ and $\epsilon/(m_e c^2)$. The speed of light and elementary charge are set to unity. When we refer to the electron–ion case (e–i), the ions are assumed to be motionless ($m_i \to \infty$ limit). To keep the notations consistent, electron quantities come with a subscript e, while ion and positron quantities come with a subscript p.

By our choice of polarisation and direction of magnetic field, quantity a_e is always positive, while a_p can have either sign. This is related to the possibility of cyclotron resonance: by the choice of polarisation, it is the positively charged particles (positrons) that can be in resonance. Below we refer to them as 'resonant particles' – this term is related to the type of particles, not particular particles that are in resonance.

Given our choice of polarisation, $|\chi_p| > \chi_e$. Thus, superluminal waves correspond to $\chi_p < 0$, while subluminal waves correspond to $\chi_p > 0$.

3. Basic linear plasma waves propagating along magnetic field

As we are interested in relativistic modifications, let us briefly review the conventional linear case (e.g. Akhiezer *et al*. 1975), see figure 1, in which case fluctuating quantities and dispersion relation are

$$\begin{aligned}
v_{0,e} &= a_0 \frac{\omega}{\omega + \omega_B}, \\
v_{0,p} &= a_0 \frac{\omega}{\omega_B - \omega}, \\
|v_{0,p}| &> v_{0,e}, \\
r_p = \frac{|v_{0,p}|}{\omega} &> r_e = \frac{|v_{0,e}|}{\omega}, \\
n^2 - 1 = -\left(\frac{1}{\omega\,(\omega_B - \omega)} + \frac{1}{\omega\,(\omega_B + \omega)} \right) \omega_p^2 &\overset{\text{pairs}}{\to} \frac{2\omega_p^2}{\omega_B^2 - \omega^2},
\end{aligned} \tag{3.1}$$

where $r_{e,p}$ are corresponding Larmor radii. In (3.1), we explicitly separated contributions from resonant and non-resonant particles. The final expression, after $\to$ sign, is for a pair plasma. Notice that at $\omega > \omega_B$ velocities of particles are counter-aligned with respect to each other, so that their currents add, while for $\omega < \omega_B$ velocities of particles are aligned so that their currents subtract. For definiteness, we label the direction of rotation with respect to non-resonant particles, so that 'co-rotating resonant particles' means the velocities of two species are aligned (in the linear case, this occurs for $\omega_B > \omega$; see (3.1)).

https://doi.org/10.1017/S0022377826101342 Published online by Cambridge University Press

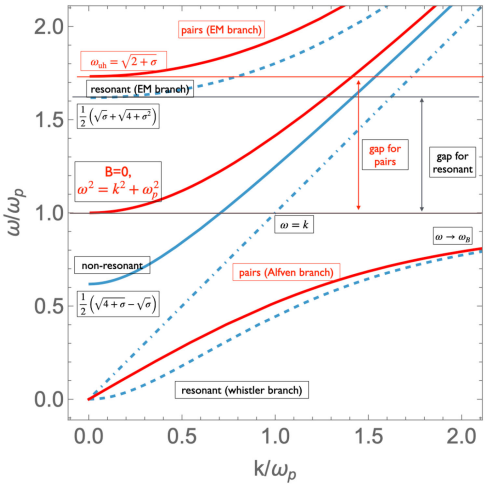


FIGURE 1. Dispersion relations for linear waves for particular choice $\sigma \equiv (\omega_B/\omega_p)^2 = 1$.

The subluminal branches, whistler and/or Alfvén, extend to $0 < \omega < \omega_B$. At small $\omega \ll \omega_B$,

$$\omega = \frac{k^2\omega_B}{\omega_p^2}, \qquad \text{whistlers},$$
$$\frac{k^2}{\omega^2} = 1 + \frac{2\omega_p^2}{\omega_B^2} = 1 + \frac{2}{\sigma}, \quad \text{Alfvén}, \tag{3.2}$$

where

$$\sigma = \frac{\omega_B^2}{\omega_p^2} \tag{3.3}$$

is the magnetisation parameter (Kennel & Coroniti 1984).

Superluminal branches have a cutoff at

$$\omega_{\rm uh} = \sqrt{\omega_B^2 + 2\omega_p^2} = \sqrt{2+\sigma}\,\omega_p, \qquad \text{pairs, upper hybrid frequency},$$
$$\omega = \frac{1}{2}\left(\frac{\omega_B}{\omega_p} + \sqrt{4 + \frac{\omega_B^2}{\omega_p^2}}\right) = \frac{1}{2}(\sqrt{4+\sigma} + \sqrt{\sigma})\omega_p, \text{ resonant EM branch},$$
$$\omega = \frac{1}{2}\left(\sqrt{4 + \frac{\omega_B^2}{\omega_p^2}} - \frac{\omega_B}{\omega_p}\right) = \frac{1}{2}(\sqrt{4+\sigma} - \sqrt{\sigma})\omega_p, \text{ non-resonant EM branch}. \tag{3.4}$$

Various particles' trajectories and forces are sketched in figure 2 (equal masses are assumed). There are two forces acting on a particle: electric field of the wave E_w and the Lorentz force from the guide field $v_{e,p}B_0$. For non-resonant particles, both forces add. For resonant particles they subtract: for $\omega > \omega_B$ the force from the electric field is larger, while for $\omega < \omega_B$ the Lorentz force dominates.

https://doi.org/10.1017/S0022377826101342 Published online by Cambridge University Press

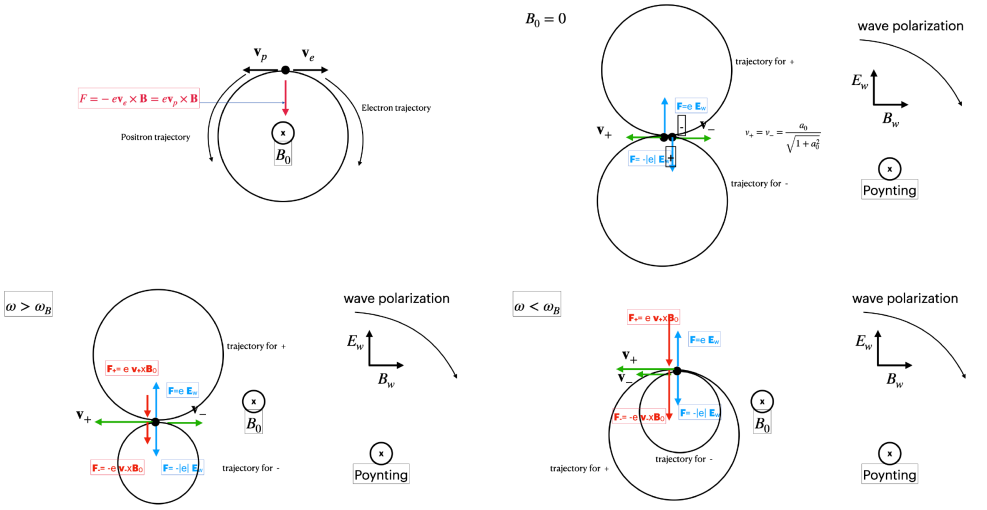


FIGURE 2. Particle trajectories in CP EM waves propagating along the magnetic field. Top left: in external magnetic field without the wave; top right: in EM wave without guide magnetic field. In both cases at each point velocities of oppositely charged particles are counter-aligned (so the currents add). Bottom row shows trajectories in magnetic field. Left: weak magnetic field (velocities counter-aligned, currents add); right: strong magnetic field (velocities aligned, currents subtract).

4. Single-particle motion in nonlinear CP EM wave with guide field

For the CP wave, the dispersion relations and force balance equations separate. This allows fully nonlinear treatment. We first consider single-particle dynamics in the presence of a CP wave and guide magnetic field (propagation along the field). For now, the frequency of the wave ω is considered as given. In plasma, § 5, the wave frequency in the gyration frame has to be calculated self-consistently.

A special type of solution (not a general one starting with arbitrary initial conditions) involves particle velocities instantaneously (counter-)aligned with the wave's magnetic field. The force balance can be written in a fairly compact form:

$$\gamma_\pm m_e v_\pm \omega = e(E_w \pm v_\pm B_0), \tag{4.1}$$

where $\pm$ accounts for two directions of the background field/charge/polarisation sign (speed of light is set to unity). But different realisations are fairly complicated depending on the values of the wave electric field, guide B_0 and wave frequency ω. They are illustrated in figure 2.

Momenta of non-resonant a_e (dot–dashed lines in figure 3) are positive $a_e > 0$ by our choice of polarisation. Dependence of a_e on parameters is fairly straightforward.

The most interesting case is for particles that may be in resonance. (Recall that, in the linear case, $a_0 = a_p(f_B - 1)$, the resonance is reached at $f_B = 1$. Below the resonance $a_p < 0$ (counter-aligned with non-resonant particles), while above the resonance $a_p > 0$ (aligned).)

Nonlinear effects make the most important modifications for particle trajectories near the resonance $f_B \approx 1$. Formally, the resonance shifts from $f_B = 1$ to

$$a_p = \sqrt{f_B^2 - 1}. \tag{4.2}$$

But, in fact, it is never reached, as we discuss next.

https://doi.org/10.1017/S0022377826101342 Published online by Cambridge University Press

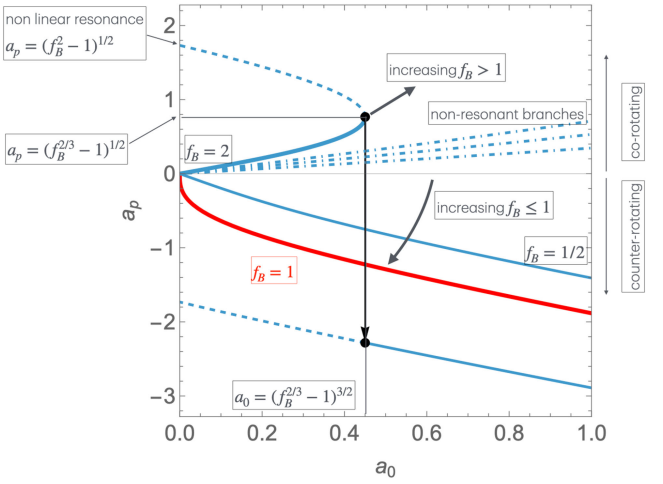


FIGURE 3. Particle momenta in nonlinear CP waves. For $\omega \geqslant \omega_B$ ($f_B = \omega_B/\omega \geqslant 1$, including the case $\omega = \omega_B$), resonant particles are counter-rotating (negative χ_p). For $\omega < \omega_B$, resonant particles are co-rotating for mild $a_0 \leqslant (f_B^{2/3} - 1)^{3/2}$ and counter-rotating for larger a_0. Dashed branches are likely to be unstable.

First, consider a special case $f_B = 1$ (thick line in figure 3). In this case, momentum is determined from

$$a_0 = \tanh(\chi_p) - \sinh(\chi_p). \tag{4.3}$$

This is an equation for $\chi_p(a_0)$. Since $a_0 > 0$ by definition, negative χ_p is needed (resonant particles are still counter-aligned with non-resonant particles, just like for $f_B < 1$).

For small a_0,

$$a_p = -(2a_0)^{1/3}. \tag{4.4}$$

Thus, for the special case $f_B = 1$ particle motion is not a linear response to wave intensity in the small $a_0 \ll 1$ limit. For any $f_B \neq 1$, the response is linear, $|a_p| \propto a_0$ in the limit $a_0 \to 0$.

The situation slightly above the resonance, $f_B \geqslant 1$, is more complicated:

(i) At mild intensities, $a_0 \leqslant a_0^{(\mathrm{crit})} = (f_B^{2/3} - 1)^{3/2}$, there are three branches for the solution $a_p(a_0)$. The physical one (least energy of a particle and correct limit for $a_0 \to 0$) is co-rotating – positive χ_p (thick curve in figure 3, near $f_B = 2$ box). Thus, the synchrotron resonance (4.2) is located on the upper curve, and hence is never reached. (We encounter here a mathematical oddity: a formal solution for forced oscillations $a_p(a_0)$ connects to free oscillations $\omega = \omega_B/\gamma_p$ at $a_0 = 0$.) The nonlinear cyclotron resonance (4.2) corresponds to particles gyrating without a wave. Hence, this point does not reflect a response of plasma to an EM perturbation – it is an initial condition on particle velocities.

(ii) At intensities $a_0 \geqslant a_0^{(\mathrm{crit})}$ there is only one counter-rotating branch (solid curve at bottom right in figure 3). Thus, for fixed $f_B > 1$ (below cyclotron resonance) and increasing a_0 there is a transition (indicated by a vertical arrow) from a co-rotating to a counter-rotating state. Since counter-rotating states correspond to superluminal waves, for a given a_0 there are no subluminal waves beyond some k.

https://doi.org/10.1017/S0022377826101342 Published online by Cambridge University Press

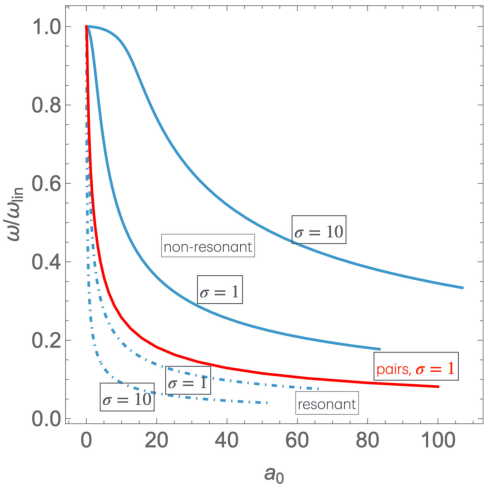


FIGURE 4. Nonlinear cutoff frequencies, as a ratio to linear ones, (3.4). In all cases, cutoff frequencies decrease with large a_0.

5. Relativistically nonlinear CP EM waves in magnetised plasma

Next, we finally turn to the properties of nonlinear EM waves in a pair plasma. Above, in § 4, we considered frequency as given. It is, in fact, determined by the properties of the plasma.

An additional complication comes from the arbitrary dependence of wave intensity on frequency: $a_0(\omega)$ is a free parameter. Generally, the dispersion relation has the form

$$\omega = \omega(k, a_0(\omega)). \tag{5.1}$$

Various $a_0(\omega)$ will produce different dispersions $\omega(k)$.

In what follows, we first consider an exemplary case of constant $a_0(\omega)$. It highlights the key point: relativistically nonlinear subluminal modes terminate at some $\omega^*{-}k^*$ point on the $\omega{-}k$ plane. Later, in § 5.4, we highlight general relations and discuss the case of constant ratio E_w/B_0 (wave intensity to guide field).

The cases of single components and pair plasma are somewhat different. For the single-component case, the mathematics is simpler: eliminate particle momenta from the force balance, and use it in the expression for $n^2 - 1$. In a pair plasma, the procedure is more complicated: particle momenta $a_{e,p}$ both depend on the resulting wave frequency.

5.1. *Superluminal modes*

Superluminal modes have $\chi_p < 0$. All superluminal modes (R, L and Alfvén) have cutoffs at (figure 4)

$$\omega^2_{\rm cut} = \frac{\tanh \chi_e - \tanh \chi_p}{a_0} \omega_p^2. \tag{5.2}$$

https://doi.org/10.1017/S0022377826101342 Published online by Cambridge University Press

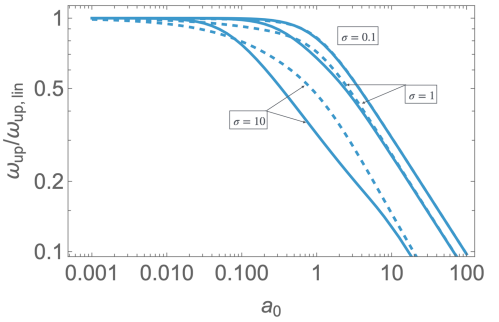


FIGURE 5. Nonlinear cutoff frequencies, as a ratio to linear ones. Solid lines are solutions of (3.4), dashed lines are approximations (5.5). In all cases, cutoff frequencies decrease with large a_0.

For the single-component cases, these relations can be resolved analytically. The resonant ($\chi_p < 0$) case is

$$\omega_{\rm cut}^2 = \frac{\tanh|\chi_p|)}{a_0}\omega_p^2 = \frac{\omega_p^2}{\cosh(\chi_p) - f_B} = \frac{1}{2}\mathrm{sech}(\chi_p)\left(\sqrt{\omega_B^2 + 4\omega_p^2\cosh(\chi_p)} + \omega_B\right),$$
$$a_0 = f_B\tanh(\chi_p) - \sinh(\chi_p) = \sinh(\chi_p)\left(\frac{2\omega_B}{\sqrt{\omega_B^2 + 4\omega_p^2\cosh(\chi_p)} + \omega_B} - 1\right). \quad (5.3)$$

The non-resonant case is

$$\omega_{\rm cut}^2 = \frac{\tanh\chi_e}{a_0}\omega_p^2 = \frac{\omega_p^2}{\cosh(\chi_e) + f_B} = \frac{1}{2}\mathrm{sech}(\chi_e)\left(\sqrt{\omega_B^2 + 4\omega_p^2\cosh(\chi_e)} - \omega_B\right),$$
$$a_0 = f_B\tanh(\chi_e) + \sinh(\chi_e)$$
$$= \frac{\omega_B\tanh(\chi_e)\left(\sqrt{\omega_B^2 + 4\omega_p^2\cosh(\chi_e)} + \omega_B\right)}{2\omega_p^2} + \sinh(\chi_e) \quad (5.4)$$

(compare with (8.1.4.2) in Akhiezer *et al*. (1975)).

For a pair plasma, the cutoff frequencies cannot be put into a compact expression. A good approximation is achieved if we use

$$\omega_B \to \omega_B/\left(1 + a_0^{2/3}\right)^{3/2},$$
$$\omega_p \to \omega_p/\left(1 + a_0^2\right)^{1/4} \quad (5.5)$$

(see figure 5). The relation for ω_p is exact for the $\omega_B = 0$ case (Akhiezer & Polovin 1956).

In figure 6, we plot dispersion curves for superluminal modes. Qualitatively, the curves look similar to those of the linear case, with cutoff frequencies shifted down for large a_0.

https://doi.org/10.1017/S0022377826101342 Published online by Cambridge University Press

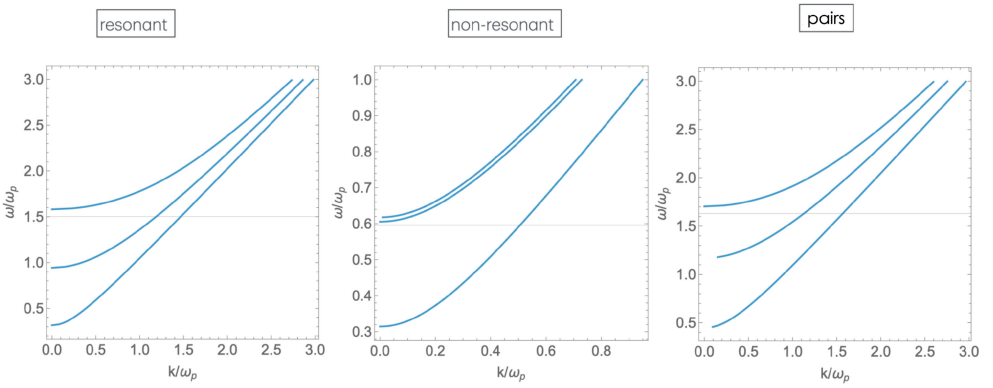


FIGURE 6. Dispersion curves for superluminal modes for $\sigma = 1$, $a_0 = 0.1,\ 1,\ 10$ (top to bottom).

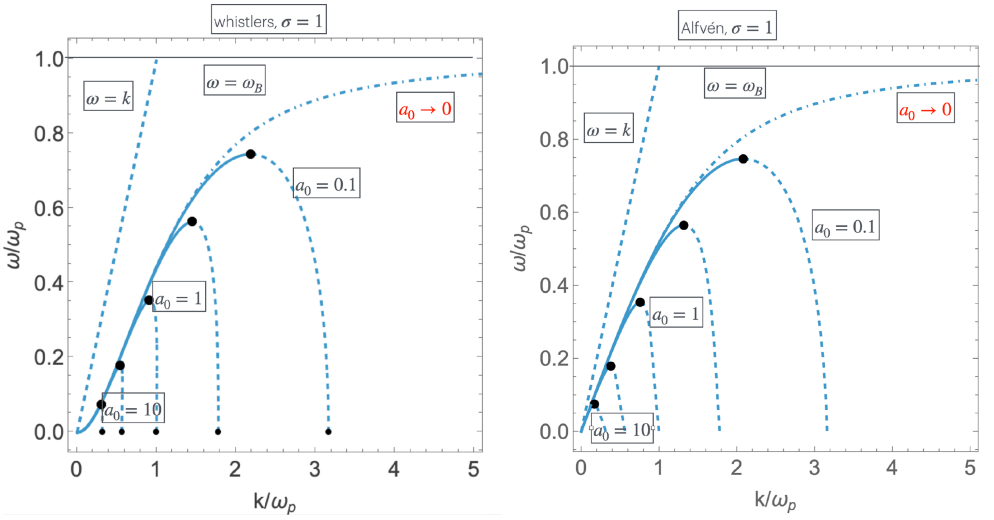


FIGURE 7. Dispersion curves for relativistically nonlinear whistler (left panel) and Alfvén (right panel) waves, $\sigma = 1$. Dispersion curves experience a bend at finite $k^*{-}\omega^*$; above this point, resonant particles are on the upper branch in figure 3. Dispersion curves terminate at $\omega = 0$, $k_{\max} = \omega_p/\sqrt{a_0}$ (lower row of points).

5.2. *Subluminal modes*

There are two types of subluminal modes: whistler (single-component, resonant) and Alfvén (pairs) modes; there are no subluminal modes corresponding to single-component non-resonant particles.

A qualitatively new effect appears for subluminal modes – bend of the dispersion relation at finite $\omega^*{-}k^*$ (figure 7). At the bend, the group velocity $v_g = \partial\omega/\partial k$ becomes zero. Above the bend (at higher k), the group velocity is negative.

Recall that subluminal modes correspond to $f_B \geqslant 1$, while the resonant component has $\chi_p \geqslant 0$. With increasing a_0 it follows the middle branch in figure 3. The middle

https://doi.org/10.1017/S0022377826101342 Published online by Cambridge University Press

branch $a_p(a_0)$ terminates at some finite a_0. The critical point corresponds to

$$\omega^* = \frac{\omega_B}{\left(1+a_0^{2/3}\right)^{3/2}} \to \frac{\omega_B}{a_0} \tag{5.6}$$

(the latter relation is for $a_0 \gg 1$). It is the same for both whistler and Alfvén modes.

For fixed $a_0(\omega) = \text{const.}$, dispersion curves bend over in the $\omega{-}k$ plane at some finite values of $\omega^*{-}k^*$, and since above the bend modes are likely to be unstable, the dispersion curve effectively terminates. At frequencies well below the cyclotron frequency, $f_B \gg 1$, Alfvén waves exist only for $\omega \leqslant \omega_B/a_0$, or reverting to the fields,

$$E_w \leqslant B_0 \tag{5.7}$$

(see § 5.4).

For single-component plasma (relativistically nonlinear whistler modes), the corresponding wave vector and phase velocities are

$$\begin{aligned} k^2 &= \omega^2 - \frac{\omega\omega_p^2}{\omega\sqrt{1+a_p^2} - \omega_B}, \\ k^{*,2} &= \frac{\omega_B^2}{\left(1+a_0^{2/3}\right)^3} + \frac{\omega_p^2}{\sqrt{1+a_0^{2/3}}\,a_0^{2/3}}, \\ v^{*,2} &= \frac{a_0^{2/3}\sigma}{a_0^{2/3}\sigma + \left(1+a_0^{2/3}\right)^{5/2}} \to \frac{\sigma}{a_0+\sigma}, \end{aligned} \tag{5.8}$$

where v^* is the terminal phase velocity of whistler modes (figure 7, left panel).

For relativistic whistler modes, the maximal phase velocity is reached at

$$\begin{aligned} a_0 &= (2/3)^{3/2} = 0.544, \\ v^*_{\max} &= \sqrt{\frac{\sigma}{\sigma + 25\sqrt{(5/3)}/6}}, \\ \gamma^{*,2} &= 1 + \frac{6}{25}\sqrt{\frac{3}{5}}\sigma. \end{aligned} \tag{5.9}$$

The dispersion curve ends at $\omega = 0$, $k_{max} = \omega_p/\sqrt{\alpha_0}$ (lower row of points in figure 7).

In a pair plasma k^* (terminal wave vector for relativistically nonlinear Alfvén waves) has to be found numerically (figure 7, right panel).

In figure 8 we plot terminal Alfvén velocities as a function of a_0 for different magnetisations. For comparison, in dashed lines we show linear Alfvén speed for $\omega \to 0$, $v_A = \sqrt{\sigma/(2+\sigma)}$ (the factor 2 accounts for two species; σ is defined with respect to each separately). Relativistically nonlinear Alfvén waves are slower due to increasing effective mass.

https://doi.org/10.1017/S0022377826101342 Published online by Cambridge University Press

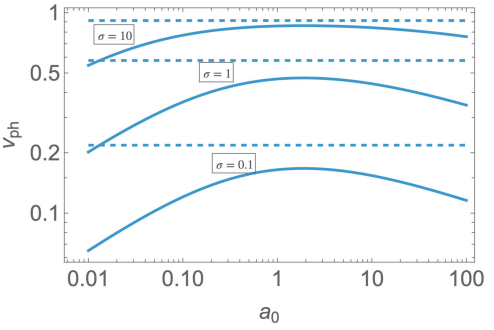


FIGURE 8. Terminal phase velocities for Alfvén waves, $\sigma = 1$. Dashed lines are linear limits for $k \to 0$, $v_A = \sqrt{\sigma/(2+\sigma)}$.

5.3. *Negative group velocity branch and the bend in $\omega(k)$*

Negative group velocity branches, at $k > k^*$, are likely to be unstable. The stability criterion for linear waves (Landau & Lifshitz 1960, pp. 80 and 84) is violated:

$$\partial_\omega(\omega\epsilon(\omega)) = -n^2 - 2n(\partial_k\omega)^{-1} < 0. \tag{5.10}$$

This indicates that the wave has negative energy and is likely to become unstable by coupling to the positive energy modes. Negative energy of the wave indicates that the wave would take energy from the plasma components.

As figure 3 indicates, at any given a_0, the upper branch has particles with larger momenta than the lower branch. It is an interesting coincidence that dispersion curves, which describe the response of a medium to a perturbation, terminate at free-rotating particles.

As another argument in favour of instability of a branch above $k > k^*$, the terminal point $\omega = 0$, $k \neq 0$ corresponds to the conditions for electron cyclotron maser/gyrotron instability (Melrose 1989), with the exception that in a pair plasma both components have distribution in perpendicular momenta $\propto \delta(a_{e/p} - p_{0,e/p})$. This clearly indicates population inversion and instability. Finally, negative group velocity is possible in media with inverted populations, and hence unstable (Garrett & McCumber 1970).

In passing, we note that there are in fact media where the phase and group velocities of EM waves are oppositely directed: they go under the name left-handed media or negative-index metamaterials (Veselago 1968). The difference is that experimental set-ups with $n < 0$ are fixed, while here they are dynamic. Another prominent case when phase and group velocities are counter-aligned is the Cherenkov emission (e.g. Bolotovskii & Stolyarov 1975).

5.4. *Dispersion relations for arbitrary $\eta_w = E_w/B_0$*

Above, we considered a case of constant $a_0(\omega) \equiv a_0$, and hence increasing wave electric field $E_w(\omega) \propto \omega$. We found that Alfvén wave dispersion terminates at $E_w \sim B_0$. Next, we discuss generation properties of the dispersion relation, and repeat calculations for arbitrary $\eta_w = E_w/B_0$.

https://doi.org/10.1017/S0022377826101342 Published online by Cambridge University Press

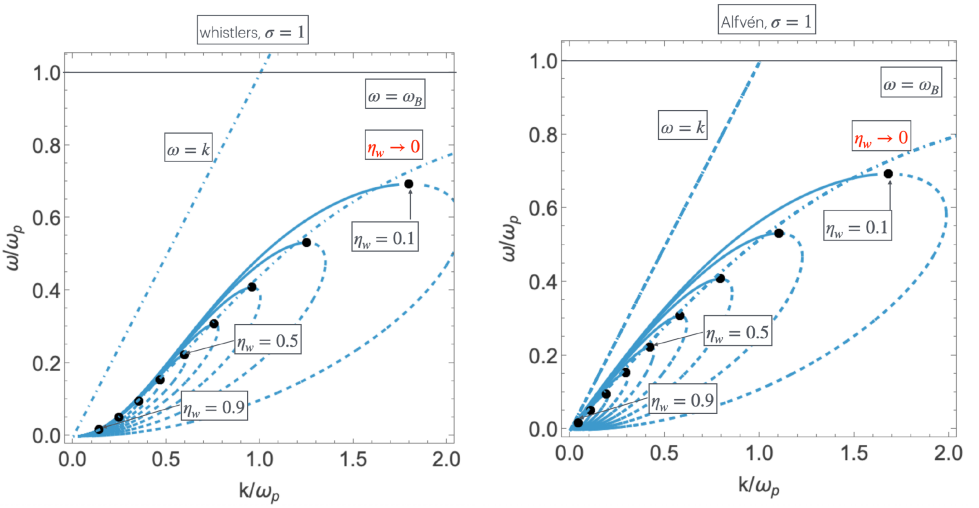


FIGURE 9. Same a figure 7, assuming constant ratio of wave intensity to guide field $\eta_w = E_w/B_0$.

Instead of (2.7), for given η_w we find

$$n^2 - 1 = \left(\frac{a_p}{\sqrt{1+a_p^2}} - \frac{a_e}{\sqrt{1+a_e^2}}\right)\frac{1}{\eta_w}\frac{\omega_p^2}{\omega\omega_B} = \left(\tanh\chi_p - \tanh\chi_e\right)\frac{1}{\eta_w}\frac{\omega_p^2}{\omega\omega_B},$$

$$\eta_w = \left(\frac{1}{\sqrt{1+a_p^2}} - \frac{\omega}{\omega_B}\right)a_p = \tanh\chi_p - \frac{\sinh\chi_p}{f_B},$$

$$\eta_w = \left(\frac{1}{\sqrt{1+a_e^2}} + \frac{\omega}{\omega_B}\right)a_e = \tanh\chi_e + \frac{\sinh\chi_e}{f_B}. \tag{5.11}$$

For frequency-dependent $\eta_w(\omega)$, the relation (5.6) for the critical frequency, where dispersion of subluminal modes terminates, can be written as

$$\tilde{\omega}^* = \frac{\omega^*}{\omega_B} = \left(1 - (\eta_w)^{2/3}\right)^{3/2},$$

$$a_p^* = \sqrt{\frac{1}{\tilde{\omega}^{*,2/3}} - 1} = \frac{\eta_w^{1/3}}{\sqrt{1-\eta_w^2}},$$

$$\eta_w(\omega) = \frac{E_w(\omega)}{B_0}. \tag{5.12}$$

In figure 9 we plot the dispersion curves for relativistically nonlinear subluminal waves assuming a constant ratio of wave intensity to guide field $\eta_w = E_w/B_0$. With increasing η_w, propagating waves are confined to smaller corner near $\omega,\ k \approx 0$. For $\eta_w \geqslant 1$ waves cannot propagate.

Relation (5.12) highlights the universal relationship: when at a given frequency the intensity of the fluctuating field in a subluminal wave exceeds the guide field, $\eta_w \to 1$, the wave cannot propagate.

https://doi.org/10.1017/S0022377826101342 Published online by Cambridge University Press

5.5. *Finite ion mass*

In the case of finite mass of the ion component, $\mu = m_p/m_e \neq 1, \infty$, general relations are much more complicated, as two new frequencies appear (ion cyclotron and ion plasma), both modified by the nonlinear effects. To achieve relativistic motion of ions in unmagnetised plasma, a wave should be $a_0 \sim \mu = 1836$ (a_0 is defined with respect to the electron mass).

Introduction of a guide field leads to a number of complications. Here the form (5.11) provides a better insight. First, the equation for plasma response involves ω_p^2/ω_B and is thus mass-independent. Mass dependence enters through dynamical equations for velocities of the two components.

As we discussed above, the most important point is the fairly subtle near-cyclotron-resonance behaviour. Two cases can then be identified: CP waves that can resonate with electrons (typically called R-modes), and waves that can resonate with ions (L-modes). The R-modes are well described by the infinite mass limit considered above.

For L-modes, relation (5.12) for the critical frequency, where dispersion of subluminal modes terminates, can be written as

$$\begin{aligned} \tilde{\omega}_i^* &= \frac{\omega^*}{\omega_{B,i}} = \frac{\omega^*}{\omega_B}\mu = \left(1-(\eta_w)^{2/3}\right)^{3/2}, \\ a_p^* &= \sqrt{\frac{1}{\tilde{\omega}_i^{*,2/3}}-1} = \frac{\eta_w^{1/3}}{\sqrt{1-\eta_w^2}}, \\ \omega_{B,i} &= \frac{\omega_B}{\mu} \end{aligned} \tag{5.13}$$

(the physical momentum of ions now is μa_p).

An admixture of ions can have a disproportionally large effect, as it introduces an additional low-frequency resonance. But calculating the properties of the dispersion relation would require separate 'tour de force' calculations.

6. Discussion

In this paper, we considered relativistically nonlinear CP waves propagating along a magnetic field. We were able to solve the system exactly, nonlinearly relativistic. These exact relations provide guidance to more general setups.

Dispersion curves for single-component plasmas (two possible polarisations) and pair plasmas were investigated. For superluminal modes, the modifications from the linear case are qualitative: decreasing cutoff frequencies.

The most interesting effect appears for subluminal modes: dispersion curves effectively terminate at some finite values of ω^*-k^*. At which point the group velocity becomes zero. At this point, the fluctuating electric field of the wave becomes equal to the guide magnetic field.

Though the effect reminds one of charge starvation – it is not. The critical point is independent of plasma density, as illustrated by figure 10.

The effect we observe is a variant of zero group velocity. Waves at the zero group velocity frequency are stationary and do not propagate energy over a long distance; instead, the energy remains localised near the source, forming a standing wave.

In astrophysical applications, condition (5.7) (or equivalently $\eta_w = 1$, (5.12)) may be reached for waves propagating in the dipolar field of magnetar magnetospheres.

https://doi.org/10.1017/S0022377826101342 Published online by Cambridge University Press

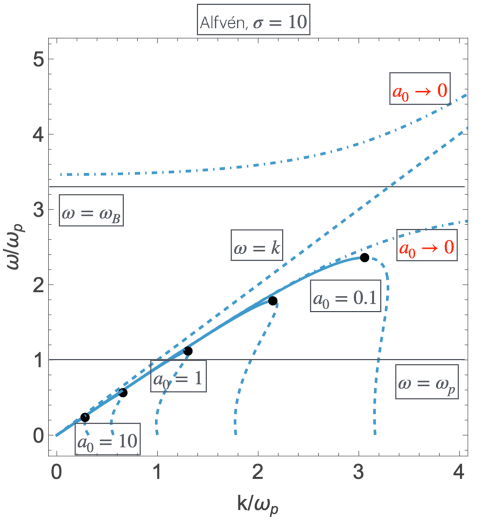


FIGURE 10. Dispersion curves for $\sigma = 10$. Compare with figure 7. This illustrates that the critical point is independent of the density.

At smaller radii, $B_0 \gg E_w$, but since $B_0 \propto r^{-3}$ while $E_w \propto r^{-1}$, condition (5.7) then can be reached within the magnetosphere. Instead of propagation, the waves will pile up near the critical point. As a result the wave will 'open' the magnetosphere (Sharma, Barkov & Lyutikov 2023). The energy of the wave will be spent on distorting the magnetosphere, which will then recover on a long resistive time scale.

In a pair plasma, in the linear regime, there is a gap in dispersion relations for $\omega_B^2 \leqslant \omega^2 \leqslant \omega_B^2 + 2\omega_p^2$. In the relativistic regime, there is still a gap:

$$\frac{\omega_B^2}{\left(1+a_0^{2/3}\right)^3} \leqslant \omega^2 \leqslant \frac{\omega_B^2}{\left(1+a_0^{2/3}\right)^3} + 2\frac{\omega_p^2}{\sqrt{1+a_0^2}} \tag{6.1}$$

(upper limit is approximate). The width of the gap becomes smaller at large a_0:

$$\Delta\omega \sim \sqrt{2}\frac{\omega_p}{\sqrt{a_0}}. \tag{6.2}$$

We stress that the solutions for nonlinear waves discussed here are applicable only to CP waves propagating along the magnetic field. In addition, we assumed that both species share the same gyration frame: this implicitly neglects possible effects of ponderomotive acceleration. (Electrons and positrons will experience different ponderomotive acceleration in a CP wave.)

Finally, we hypothesise that waves will become modulationally unstable before reaching the terminal point $\omega^*{-}k^*$. This is better studied with direct PIC simulation (see § 1 for discussion of numerical challenges).

Acknowledgements

This research was supported in part by grant NSF PHY-2309135 to the Kavli Institute for Theoretical Physics (KITP). I would like to thank participants at the programme 'Frontiers of Relativistic Plasma Physics' for numerous discussions. Special acknowledgments are due to T. Blackburn, T. Grismayer, P. Kovtun,

https://doi.org/10.1017/S0022377826101342 Published online by Cambridge University Press

Y. Lyubarsky, M. Medvedev, L. Silva, A. Spitkovsky, C. Thompson and M. Vranic. I would also like to thank S. Bulanov and S. Komissarov for comments on the manuscript.

Editor Luís O. Silva thanks the referees for their advice in evaluating this article.

Declaration of interests

The author declares no conflict of interests.

REFERENCES

AKHIEZER, A.I., AKHIEZER, I.A., POLOVIN, R.V., SITENKO, A.G. & STEPANOV, K.N. 1975 *Plasma electrodynamics*. Volume 1 – Linear theory. Volume 2 – Non-linear theory and fluctuations. Oxford Pergamon Press International Series on Natural Philosophy.

AKHIEZER, A.I. & POLOVIN, R.V. 1956 Theory of wave motion of an electron plasma. *Soviet Phys.-JETP* **3**, 696–705.

BELL, A.R. & KIRK, J.G. 2008 Possibility of prolific pair production with high-power lasers. *Phys. Rev. Lett.* **101**, 200403.

BELOBORODOV, A.M. 2021 Can a strong radio burst escape the magnetosphere of a magnetar? *Astrophys. J. Lett.* **922**, L7.

BOCHENEK, C.D., RAVI, V., BELOV, K.V., HALLINAN, G., KOCZ, J., KULKARNI, S.R. & MCKENNA, D.L. 2020 A fast radio burst associated with a Galactic magnetar. *Nature* **587**, 59–62.

BOLOTOVSKII, B.M. & STOLYAROV, S.N. 1975 Current status of the electrodynamics of moving media (infinite media). *Soviet Phys. Uspekhi* **17**, 875.

CHIME/FRB Collaboration *et al.* 2020 A bright millisecond-duration radio burst from a Galactic magnetar. *Nature* **587**, 54–58.

CLEMMOW, P.C. 1974 Nonlinear waves in a cold plasma by Lorentz transformation. *J. Plasma Phys.* **12**, 297–317.

CORDES, J.M. & CHATTERJEE, S. 2019 Fast radio bursts: an extragalactic enigma. *ARA&A* **57**, 417–465.

GARRETT, C.G. & MCCUMBER, D.E. 1970 Propagation of a Gaussian light pulse through an anomalous dispersion medium. *Phys. Rev. A* **1**, 305–313.

GOLBRAIKH, E. & LYUBARSKY, Y. 2023 On the escape of low-frequency waves from magnetospheres of neutron stars. *Astrophys. J.* **957**, 102.

HEYVAERTS, J., LEHNER, T. & MOTTEZ, F. 2012 Non-linear simple relativistic Alfvén waves in astrophysical plasmas. *Astron. Astrophys.* **542**, A128.

KENNEL, C.F. & CORONITI, F.V. 1984 Confinement of the Crab pulsar's wind by its supernova remnant. *Astrophys. J.* **283**, 694–709.

LANDAU, L.D. & LIFSHITZ, E.M. 1960 *Electrodynamics of Continuous Media*, Energy Conversion Management. Available at: https://ui.adsabs.harvard.edu/abs/1960ecm..book.....L.

LORIMER, D.R., BAILES, M., MCLAUGHLIN, M.A., NARKEVIC, D.J. & CRAWFORD, F. 2007 A bright millisecond radio burst of extragalactic origin. *Science* **318**, 777.

LUAN, J. & GOLDREICH, P. 2014 Physical constraints on fast radio bursts. *Astrophys. J. Lett.* **785**, L26.

LYUBARSKY, Y. 2014 A model for fast extragalactic radio bursts. *Mon. Not. R. Astron. Soc.* **442**, L9–L13.

LYUTIKOV, M. 2021 Coherent emission in pulsars, magnetars, and fast radio bursts: reconnection-driven free electron laser. *Astrophys. J.* **922**, 166.

LYUTIKOV, M., BURZAWA, L. & POPOV, S.B. 2016 Fast radio bursts as giant pulses from young rapidly rotating pulsars. *Mon. Not. R. Astron. Soc.* **462**, 941–950.

LYUTIKOV, M. & GURARIE, V. 2025 Anderson self-localization of light in pair plasmas. arXiv: 2509.20594.

MARKLUND, M. & SHUKLA, P.K. 2006 Nonlinear collective effects in photon-photon and photon-plasma interactions. *Rev. Mod. Phys.* **78**, 591–640.

MELROSE, D.B.1989 *Instabilities in Space and Laboratory Plasmas*. Available at: https://ui.adsabs.harvard.edu/abs/1989islp.book.....M.

https://doi.org/10.1017/S0022377826101342 Published online by Cambridge University Press

PETROFF, E., HESSELS, J.W.T. & LORIMER, D.R. 2022 Fast radio bursts at the dawn of the 2020s. *Astron. Astrophys. Rev.* **30**, 2.

RIDGERS, C.P., BRADY, C.S., DUCLOUS, R., KIRK, J.G., BENNETT, K., ARBER, T.D., ROBINSON, A.P.L. & BELL, A.R. 2012, Dense electron-positron plasmas and ultraintense γ rays from laser-irradiated solids. *Phys. Rev. Lett.* **108**, 165006.

SHARMA, P., BARKOV, M.V. & LYUTIKOV, M. 2023 Relativistic coronal mass ejections from magnetars. *Mon. Not. R. Astron. Soc.* **524**, 6024–6051.

TANGTARTHARAKUL, K., AREFIEV, A. & LYUTIKOV, M. 2025 Complete reflection of nonlinear electromagnetic waves in underdense pair plasmas enabled by dynamically formed Bragg-like structures. arXiv: 2509.06230.

VESELAGO, V.G. 1968 The electrodynamics of substances with simultaneously negative values of ϵ and μ. *Soviet Phys. Uspekhi* **10**, 509.

ZHANG, P., BULANOV, S.S., SEIPT, D., AREFIEV, A.V. & THOMAS, A.G.R. 2020 Relativistic plasma physics in supercritical fields. *Phys. Plasmas* **27**, 050601.

https://doi.org/10.1017/S0022377826101342 Published online by Cambridge University Press